

Full length article

## On the prediction of low-cost high entropy alloys using new thermodynamic multi-objective criteria

A.E. Gheribi <sup>a</sup>, A.D. Pelton <sup>a</sup>, E. Bélisle <sup>a</sup>, S. Le Digabel <sup>b</sup>, J.-P. Harvey <sup>a,\*</sup><sup>a</sup> Centre for Research in Computational Thermochemistry (CRCT), École Polytechnique de Montréal, Department of Chemical Engineering, C.P. 6079, Succ. Centre-Ville, Montréal, QC, H3C 3A7, Canada<sup>b</sup> Département of Industrial Engineering, École Polytechnique de Montréal and GERAD, C.P. 6079, Succ. Centre-ville, Montréal, QC, H3C 3A7, Canada

## ARTICLE INFO

## Article history:

Received 5 June 2018

Received in revised form

21 August 2018

Accepted 1 September 2018

Available online 6 September 2018

## ABSTRACT

In an attempt to identify new low-cost metallic materials with interesting thermo-physical properties from the Fe-Cr-Mn-Ni-V-Ti-Al- (Co-Mo) system, we present here an original tool for the design of first-generation High Entropy Alloys (HEAs). The composition of potential HEAs is calculated under a set of non-smooth and non-linear constraints and multi-objective functions linked to the single-phase start temperature, the room-temperature driving force for phase assemblage evolution and the solidification range. These are all new thermodynamic criteria for the design of HEAs. This tool links a constrained Gibbs energy minimization algorithm that uses accurate thermodynamic databases to an optimization algorithm implemented for solving “blackbox” objective functions and constraints. As a result of this work, we have identified entire sets of new FCC and BCC first-generation HEAs potentially suitable for future industrial applications. The proposed methodology is also successfully applied to identify two-phase heavily alloyed materials.

© 2018 Acta Materialia Inc. Published by Elsevier Ltd. All rights reserved.

### 1. Introduction

The design of the optimal material for a given application is a challenging task: the optimized chemistry is often obtained as a result of a complex trial and error process of the simultaneous tuning of the corrosion properties, specific mechanical properties and cost. In most cases, the ideal alloying element that improves one property might simultaneously have a detrimental effect on another. Cr in steel is a perfect example: its presence increases the corrosion resistance by the formation of a Cr<sub>2</sub>O<sub>3</sub> passivation layer at the surface of the steel [1] but stabilizes the less desirable BCC-ferrite solid solution. To solve this issue, Ni is typically added to stainless steels in order to enlarge the stability of the FCC-austenite region at high temperature at the expense of a cost increase of the resulting material.

Traditionally, researchers and scientists have explored different types of metallic alloys with addition of elements in low concentration. It appears from a review of the recent literature [2] that another alloy design strategy is starting to emerge. This strategy involves the massive addition of a high number of alloying

elements. This type of material was originally called High Entropy Alloys (HEAs) in reference to the high configurational entropy associated with the resulting disordered multicomponent solid solution.

Theoretically, these new materials appear to share common features: a sluggish diffusion of the elements which inhibits the precipitation of ordered compounds at low temperature; high local distortions of the host lattice induced by the size mismatch of the various elements which potentially strengthen the disordered solid solution; and a cocktail effect, i.e. the superposition of physico-chemical effects induced by the individual elements [3].

HEAs are often defined as metallic alloys, consisting of a single disordered solid solution (usually FCC or BCC), constructed with equal or nearly equal quantities of five or more elements. The original principle of HEA design is simple: it consists in finding an alloy made of 5 elements or more for which there is a certain domain of composition and temperature where only a single solid solution phase is stable, as opposed to multiphase systems containing a significant amount of intermetallics. In this work we define single-phase disordered solid solution materials as first-generation high-entropy alloys.

The original strategy for developing high entropy alloys evolved rapidly because of various thermochemical and mechanical

\* Corresponding author.

E-mail address: [jean-philippe.harvey@polymtl.ca](mailto:jean-philippe.harvey@polymtl.ca) (J.-P. Harvey).

shortcomings of single-phase disordered solutions. A refinement of the design strategy led naturally towards the synthesis of multiphasic materials. An adequate name for this new class of materials could be *heavily alloyed materials*. The original constrained optimization problem, i.e. maximizing the configurational entropy of mixing in order to generate a disordered single phase material for a given temperature range, has been shifted towards more complex constrained multi-objective problems that we would like to explore in this work.

Several potential first-generation HEAs with equiatomic fractions (HEAs-EAF) have already been identified in the literature [4,5]. They were mostly found by the exploration of the chemical composition space of high-order systems using thermodynamic calculations. More recently, first-principle calculations of high-entropy-alloys were presented by Feng et al. [6]. This elegant work highlighted the possibility of successfully designing alloys using a series of Density Functional Theory (DFT) calculations for the Cr-Mo-Nb-V quaternary system coupled with classical thermodynamic calculations. DFT calculations are used in this case to parameterize Gibbs energy functions of potentially stable phases for this system. Finally, experiments are performed *a posteriori* for these HEAs candidates as a final step of the design process. This design alloy strategy greatly limits the number of material syntheses necessary to find optimal HEA materials.

The CALPHAD method [7] has shown its strength over the years when exploring phase equilibria occurring in high-order systems, especially from a computational-cost point of view. At the moment, an active research theme regarding the design of HEAs is to find potential candidates outside of the equiatomic composition. In this work special attention will also be given to the single-phase start temperature (SPST). For HEAs, reducing the SPST as much as possible is highly desirable as it will minimize the thermal activation energy available for solid-solid phase transitions to occur below this temperature.

Fu et al. [8] recently proposed a classification of elements that can potentially be used for real industrial applications based on the price of raw materials and also supply viability. They concluded that the low cost ( $\leq 0.5$  USD per mole) and available (at least for more than 50 years) elements which could be sustainable for industrial manufacturing are:

$$E = \{ \text{Al, Cr, Cu, Fe, Mg, Mn, Ni, Pb, Sb, Si, Ti, V, Zn} \}$$

The goals of the present work are as follows:

- Propose an original tool for the design of **low-cost** (i.e based on chemical elements belonging to the ensemble  $E$ ) first-generation HEAs, including those with non-equiatomic fractions (HEA-NEAF). Define new multi-objective functions for the design of heavily alloyed materials based on 1) the thermodynamic room temperature driving force of phase assemblage evolution, i.e.  $\Delta G^*$ , defined as the Gibbs free energy difference (evaluated at room temperature and atmospheric pressure) between the metastable 1-phase disordered solid solution and the true equilibrium state of the system, 2) the SPST temperature, and 3) the solidification temperature range defined by the liquidus and the solidus at a given system composition, i.e. ( $T_{\text{liquidus}} - T_{\text{solidus}}$ ).
- Identify potential correlations between the optimization of these new objective functions and the amplitude of the resulting ideal configurational entropy of mixing (which is an original HEA design criterion).

Our proposed composition-phase space strategy utilises the FactSage software and its databases [9] for the equilibrium

calculations coupled to a direct search optimization method [10] to solve the constrained optimization problem.

It is to be noted here that other important constraints linked to the controlled precipitation of ordered intermetallics have been presented recently by Abu-Odeh et al. [11]. Their work on the efficient exploration of the high entropy alloy composition-phase space is based on a constraint satisfaction algorithm. In this search approach a genetic algorithm-based optimization scheme is used to expand an initial hyper-sphere that satisfies the entire set of imposed constraints. The constraints are all linked to the thermodynamic properties of a high-order system: targeted phase assemblage (single- and two-phase equilibria), targeted temperature range of phase stability and targeted type of phase transition. All these thermodynamic properties are evaluated from external calls to a constrained minimization solver as well.

As a result of the application of this strategy, the authors identified high-order phase space regions that satisfy various sets of constraints for the 5-element CoCrFeMnNi system. They presented single-phase regions that departed from the equimolar composition by at most 5% for ternary, quaternary and quinary subsystems. They also provided a more complex material design strategy to control the microstructure of a two-phase high entropy alloy belonging to the Al-CoCrFeNi system. As presented in the Appendix of this work, we can also target two-phase regions with our approach to perform a similar design of multiphasic high-entropy alloys.

The optimization scheme of Abu-Odeh et al. [11] is a constraint-type optimization method, i.e. no objective functions to be minimized and/or maximized are defined. Our approach is different, since we aim at determining specific compositions within single or two phase regions that optimize multiple objectives while respecting various constraints. This leads to the identification of optimal material candidates. Similarly to the work of Abu-Odeh et al. [11], we identify with our approach composition ranges within single- or two-phase regions. We go a step further by selecting optimal compositions based on thermodynamic-based objective functions.

As a result of this work, several potential new HEAs coming from an 8-element system are identified and discussed. This study is in line with the suggestions of Miracle and Senkov [2] on the necessity of providing high-throughput computational design techniques and new HEA criteria.

## 2. Method for predicting new HEA candidates

The conventional requirements for defining the first-generation high entropy alloys are extensively documented in the literature (see e.g. Gao et al.'s comprehensive book [5]). To design a first generation HEA, one needs conventionally to find a set of compositions where the system contains a single FCC or BCC solid solution while the ideal configurational entropy of mixing ( $\Delta S_C^{id} = -R\sum_i x_i \ln x_i$ ) is maximized [5,12]. Two additional semi-empirical criteria are also frequently used to identify, from a vast composition space, specific regions that should thermodynamically favor the formation of a single-phase disordered solid solution: i) the enthalpy of mixing of the solid solution (refs.: pure species at the temperature of interest) should lie between  $-10 \text{ kJ}\cdot\text{mol}^{-1}$  and  $+5 \text{ kJ}\cdot\text{mol}^{-1}$  to ensure its stability at low temperature and to limit the tendency of the system to form intermetallics [13], ii) the relative difference between the atomic radii of its constitutive elements and of the host lattice needs to be small enough to ensure the formation of a substitutional solid solution and to limit the tendency to form intermetallics or interstitial solutions [13]. Also, the valence electron concentration determines if the disordered solid solution will be close-packed or not, i.e FCC or BCC [14].

In the present study, the optimal compositions of HEA candidates are obtained by combining classical thermodynamic calculations performed by the FactSage software and databases [9] with the Mesh Adaptive Direct Search (MADS) optimization algorithm [10] used for the efficient exploration of the chemical and temperature phase space of the different multi-objective functions studied in this work. From a technical perspective, the most challenging constraint to satisfy in the optimization procedure is the one linked to the imposed phase assemblage. For first-generation HEAs, one needs to find a single-phase disordered solid solution (FCC or BCC). The difficulty associated with this constraint arises from the multiple discontinuities of the complex phase space of multicomponent systems as a function of both temperature and composition. To make the optimization procedure efficient and to minimize the number of equilibrium calculations required to reach an optimal solution, the single-phase constraint is treated as a sub-optimization problem. Therefore, the optimization procedure is decomposed into two steps. The first step is to find a single-phase region. To do so, we take advantage of the evaluation of the activity  $a$  of a phase performed by the FactSage software for each equilibrium calculation. The activity of a phase quantifies its thermodynamic stability with respect to the equilibrium thermodynamic state of the system: an activity lower than one implies that the phase is not thermodynamically stable under the given conditions, while an activity greater than one implies that the introduction of this phase will lower the Gibbs energy of the system. The latter scenario only occurs when the equilibrium state is not adequately identified or when a phase is deliberately excluded from the phase assemblage. Mathematically the activity is obtained by evaluating the energetic distance between the specific Gibbs energy hyperplane defining the equilibrium state of a system and the Gibbs energy of a phase not considered in the equilibrium phase assemblage. For example, the activity of a binary stoichiometric compound  $A_xB_y$ , i.e. a phase that exists only for this specific stoichiometry, is directly evaluated using the following equation:

$$a_{A_xB_y} = \exp\left(\frac{x \cdot \mu_A + y \cdot \mu_B - G_{A_xB_y}}{(x+y) \cdot RT}\right) \quad (1)$$

In this equation,  $x$  and  $y$  are the stoichiometric factors of the  $A_xB_y$  compound for the A and B species respectively,  $\mu_i$  is the chemical potential of species  $i$  in the system and  $G_{A_xB_y}$  is the total Gibbs energy of the compound. The evaluation of the activity of a solution (i.e. a phase that is potentially thermodynamically stable over a range of composition) involves the resolution of a constrained minimization problem to identify the composition of the solution that maximizes its activity. Details of the procedure are presented in the work of Harvey et al. [15].

To achieve this step in a reasonable computing time, we propose the following strategy:

#### Step 1

1. Maximize the activity  $a$  of the FCC or BCC phase until it becomes stable, i.e.  $a = 1$
2. Starting from an initial composition  $(x_0, T_0)$  for which  $a = 1$ , maximize the amount (mole fraction) of FCC or BCC until it reaches the value of 1
3. Evaluate the region around  $(x_0, T_0)$  in which the mole fraction of the single FCC or BCC phase remains equal to 1

Then, within this region:

#### Step 2a, bi-objective T-S

1. Minimize the single phase start temperature and

2. Maximize the ideal configurational entropy of mixing

or

#### Step 2b, bi-objective T-G

1. Minimize the SPST and
2. Minimize the room temperature Gibbs energy variation of the phase assemblage evolution where:  $\Delta G^* = [G(\text{single phase alloy}, 25^\circ\text{C}) - G(\text{equilibrium phase assemblage}, 25^\circ\text{C})]$

or

#### Step 2c, bi-objective T-F

1. Minimize SPST and
2. Minimize  $(T_{\text{liquidus}} - T_{\text{solidus}})$

or

#### Step 2d, multi-objective OPT

1. Minimize the SPST and
2. Maximize the ideal configurational entropy of mixing and
3. Minimize  $\Delta G^*$  and
4. Minimize  $(T_{\text{liquidus}} - T_{\text{solidus}})$

Note that the proposed methodology allows the identification of optimal compositions in distinct single-phase regions.

In our proposed search strategy, the SPST is always considered in the bi-objective function to be optimized. Step 2a is the only bi-objective function that uses the maximization of the ideal configurational entropy of mixing to identify first-generation HEAs (the conventional criterion to identify HEAs). Here, the magnitude of the ideal configurational entropy of mixing is used as a way to estimate the amount of heterogeneous pairs in the disordered solid solution. It is reasonable to assume that these heterogeneous nearest-neighbor atom pairs play a central role in the sluggish diffusion and in the solid solution strengthening effect in high entropy alloys. In fact, most of the experimental work in the literature on high entropy alloys focuses on equimolar systems, in a direct attempt to maximize the number of heterogeneous pairs in a system. The maximization of the ideal configurational entropy of mixing is also indirectly accounted for in other search strategies such as the one presented by Abu-Odeh et al. [11] as they explore chemical compositions that only slightly depart from equimolar compositions (5 % in this case).

We also acknowledge that short-range ordering always occurs in real solid solutions since the excess enthalpy induced by the formation of heterogeneous chemical bonds in a solution is never zero. As a result, disordered solutions are never true ideal solutions as heterogeneous pairs will be energetically favored. However, thermodynamic models of solid solutions that directly account for the impact of SRO on their energetic behavior such as the cluster variation method [16] or the cluster site approximation [17] are rarely used in CALPHAD-type thermodynamic databases of multicomponent system. Since the precise quantification of the SRO is not accessible from conventional thermodynamic calculations, it is reasonable to relate the number of heterogeneous pairs to the ideal configurational entropy of mixing, even though the actual entropy of mixing is not ideal.

Step 2b is a bi-objective function that minimizes the driving force for the evolution of the room temperature phase assemblage,  $\Delta G^*$ . Step 2c is a bi-objective function designed to reduce the segregation of alloying elements at grain boundaries and also in dendrites during non-equilibrium cooling. These bi-objective functions

are designed to ensure good thermal stability of the identified single-phase regions. Because entropy effects of disordered solutions become dominant at high temperature, it is of prime importance to ensure that the microstructure of these materials (which is represented in this work by the phase assemblage evaluated from classical thermodynamic calculations) does not evolve at low temperature (i.e. natural aging). As will be presented in this work, all the newly identified low-cost first-generation HEA candidates (single-phase materials) have a SPST well above 442 °C. Therefore, the equilibrium state of these materials below this temperature is multiphasic, which means they will be subject to natural aging and thus microstructural evolution. In order to minimize this aging process, we attempt to reduce as much as possible the driving force for room temperature phase assemblage evolution. Also, segregation could impact negatively on the thermal stability of some chemically heterogeneous regions.

At each iteration of the optimization process the equilibrium state is obtained from a global Gibbs energy constrained minimization performed by the FactSage software [19]. FactSage is a thermodynamic package containing different modules operated using several large and critically assessed thermodynamic and physical properties databases. In this study we have used the FSStel database [18], which is fine tuned to describe the energetic behavior of iron-containing and transition metals-based systems (except noble metals). FSStel contains data for 140 fully assessed binary, 100 ternary and 20 quaternary alloy systems. Thermodynamic properties of higher-order systems are estimated from the model parameters of the binary and ternary subsystems by various tested solution models. The database contains data for solid solution phases and for stoichiometric compounds. With the exception of Pb, Mg and Sb, for which several subsystems have not been fully integrated in the FSStel database, thermodynamic calculations performed in *E* should be reliable. An example demonstrating the robustness of the FSStel database is presented in Fig. 1. This figure shows the phase distribution as a function of temperature of an FeCrMnNiCo HEA, a material identified by Cantor et al. in 2004 [19] as an HEA candidate. The FCC disordered solid solution is found to be the only stable phase in the range 923 K  $\leq T \leq$  1523 K, and the liquidus temperature is predicted at 1584 K (Fig. 1). This is consistent with the experimental observations of Bracq et al. [20] and Otto et al. [21].

Other successful identifications of HEA candidates based on classical thermodynamic calculations [5,20,22] are clear evidence

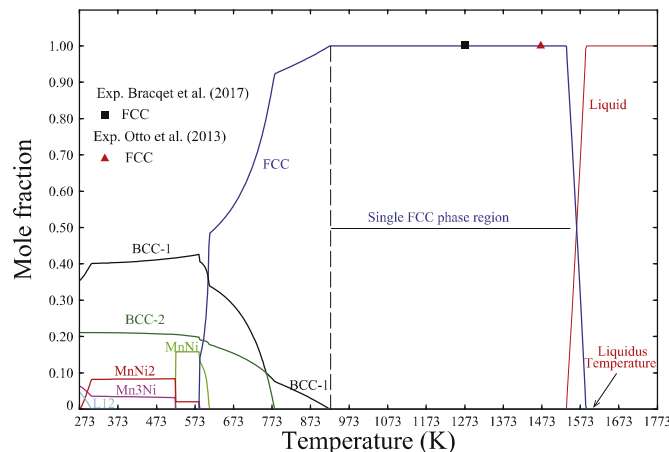


**Fig. 1.** Phase distribution as a function of temperature within the FeCrMnNiCo HEA calculated via the FactSage software and FSStel database [18]. The calculations are compared with the XRD experiments of Bracq et al. [20] and Otto et al. [21].

of the strength of this approach. However, it should be mentioned that classical thermodynamic calculations are not based on a *first-principle* method. In multicomponent systems, there is no guarantee that all the complex high-order intermetallic equilibrium phases have been introduced in the FSStel database or that all energetic interactions between hetero-atoms are accurately described for the different available solid solutions. The experimental validation of HEA candidates is therefore mandatory in most cases. The heat treatment conditions required to fully equilibrate the microstructure of the synthesized HEA candidates should be carefully selected for proper comparison with the thermodynamic calculations (i.e. avoid as-cast microstructures). When no experimental data are available, the valence electron concentration of the HEA candidate should be evaluated as its amplitude seems to be highly correlated with the type of crystal structure energetically favored for a given HEA composition [14]. It should be mentioned here that Abu-Odeh et al. also raised questions about the validity of CALPHAD databases when it comes to predictions of phase stability in central regions of the composition coordinate system. Although we cannot confirm the accuracy of the predicted phase equilibria for the entire chemical-phase space of the targeted 8-component system, the applicability of our proposed strategy to identify low-cost first-generation HEAs is not compromised as it is independent of the choice of thermodynamic database. Furthermore, the identification of new HEA candidates from this 8-component system should motivate future experimental work.

As mentioned previously, we used the Mesh Adaptive Direct Search (MADS) algorithm [23] to identify optimal system compositions. MADS generates trial compositions, sending them to FactSage for equilibrium calculations, until converging to a satisfactory or optimal composition meeting the objectives under the non-linear constraints described above. MADS has been designed for derivative-free optimization and more precisely blackbox optimization [24]. A blackbox optimization occurs when the functions defining the problem are received as outputs of a computer code seen as a blackbox. In the present case, the FactSage software is the blackbox. In this configuration, traditional gradient-based methods cannot be applied since derivatives are not available and their estimation is problematic: mainly because of noise and of the possible high computational cost required. The MADS algorithm is an iterative method generating trial points as input to the blackbox (FactSage). These points lie on a spatial discretization whose coarseness is adjusted during the course of the algorithm by a mesh size parameter. The convergence of MADS is based on the fact that eventually the mesh size goes to zero, providing a local optimum. For a detailed description of the MADS algorithm, the reader is referred to [23,24]. Several examples of its capability to solve optimization problems and several practical applications, such as alloy and process design, are presented in Refs. [25–30].

### 3. Results

#### 3.1. Validation of the numerical strategy for Co-based HEAs

We present here the HEA candidates that are obtained when considering the potential presence of Co, an expensive element not considered in our exploration of low-cost HEAs. This is a perfect benchmark to test our proposed strategy as several Co-containing HEAs have been reported in the literature [21,31–36].

One major difference between the Co-containing HEA candidates (Table 1) and the cobalt-free candidates (Table 2) is the remarkably lower SPST of the former (SPST as low as 442 °C). This results in a wide temperature range of stability for the FCC disordered solution. The optimization of the first bi-objective function (T-S) leads to the identification of 9 HEA candidates derived from

**Table 1**

Predicted Pareto optimal compositions ( $x_i$ ), single phase start temperature (SPST), ideal entropy of mixing ( $\Delta S_C^{id}$ ), room temperature Gibbs energy variation of the phase assemblage evolution ( $\Delta G^*$ ), enthalpy of mixing ( $\Delta H_{mix}^{FCC}$ ), solidus temperature ( $T_{solidus}$ ), liquidus temperature ( $T_{liquidus}$ ) and the corresponding valence electron concentration (VEC) of alloys formed of a single **FCC phase** within the **Fe-Al-Cr-Cu-Mn-Ni-V-Ti-Co** system. The compositions are in mol fraction, the temperatures are in °C, the entropy in J.mol<sup>-1</sup>.K<sup>-1</sup> and both the Gibbs energy and the enthalpy are in kJ.mol<sup>-1</sup>.

#	$x_{Fe}$	$x_{Al}$	$x_{Cr}$	$x_{Cu}$	$x_{Mn}$	$x_{Ni}$	$x_V$	$x_{Ti}$	$x_{Co}$	SPST	$\Delta S_C^{id}$	$\Delta G^*$	$\Delta H_{mix}^{FCC}$	$T_{solidus}$	$T_{liquidus}$	VEC
<b>T-S</b>																
FCo1	0.18	0.00	0.00	0.00	0.25	0.25	0.00	0.08	0.24	442	12.9	-7.1	-9.3	1068	1172	8.17
FCo2	0.16	0.00	0.08	0.01	0.24	0.24	0.05	0.00	0.22	485	14.2	-5.8	-3.2	1212	1257	8.18
FCo3	0.13	0.00	0.08	0.01	0.25	0.24	0.05	0.01	0.23	502	14.4	-5.9	-3.8	1177	1232	8.14
FCo4	0.23	0.01	0.05	0.02	0.20	0.25	0.00	0.06	0.18	542	14.6	-7.8	-7.4	1114	1220	8.15
FCo5	0.22	0.01	0.07	0.02	0.21	0.19	0.00	0.06	0.22	593	14.9	-7.9	-6.2	1097	1218	8.02
FCo6	0.22	0.03	0.03	0.04	0.19	0.23	0.00	0.06	0.20	707	15.1	-8.0	-8.4	1119	1212	8.14
FCo7	0.25	0.06	0.05	0.05	0.22	0.24	0.04	0.00	0.09	777	15.3	-7.1	-8.5	1200	1249	7.98
FCo8	0.18	0.01	0.00	0.01	0.25	0.20	0.12	0.01	0.22	627	14.2	-7.4	-4.6	1155	1201	7.95
FCo9	0.17	0.09	0.11	0.04	0.22	0.25	0.05	0.00	0.07	931	15.8	-8.4	-10.6	1154	1205	7.65
<b>T-G</b>																
FCo1	0.18	0.00	0.00	0.00	0.25	0.25	0.00	0.08	0.24	442	12.9	-7.1	-9.3	1068	1172	8.17
FCo2	0.16	0.00	0.08	0.01	0.24	0.24	0.05	0.00	0.22	485	14.2	-5.8	-3.2	1212	1257	8.18
FCo10	0.18	0.00	0.09	0.00	0.25	0.25	0.06	0.00	0.17	493	14.0	-5.6	-4.0	1205	1248	8.06
FCo11	0.25	0.00	0.18	0.00	0.00	0.25	0.07	0.00	0.25	590	12.8	-5.5	1.8	1376	1408	8.18
FCo12	0.00	0.00	0.06	0.00	0.25	0.25	0.19	0.00	0.25	705	12.7	-5.0	-3.2	1151	1179	7.81
FCo13	0.00	0.00	0.10	0.00	0.25	0.25	0.15	0.00	0.25	779	12.9	-4.6	-3.1	1160	1191	7.85
FCo14	0.00	0.00	0.25	0.00	0.25	0.25	0.00	0.00	0.25	795	11.5	-4.5	-2.3	1188	1231	8.00
<b>T-F</b>																
FCo2	0.16	0.00	0.08	0.01	0.24	0.24	0.05	0.00	0.22	485	14.2	-5.8	-3.2	1212	1257	8.18
FCo10	0.18	0.00	0.09	0.00	0.25	0.25	0.06	0.00	0.17	493	14.0	-5.6	-4.0	1205	1248	8.06
FCo15	0.22	0.01	0.05	0.00	0.25	0.24	0.09	0.00	0.14	517	14.2	-5.8	-5.3	1195	1235	7.95
FCo16	0.22	0.00	0.03	0.01	0.24	0.24	0.10	0.00	0.16	523	14.1	-5.9	-4.1	1194	1233	8.07
FCo17	0.18	0.00	0.00	0.01	0.25	0.21	0.13	0.00	0.22	552	13.5	-6.7	-3.4	1177	1212	8.03
FCo11	0.25	0.00	0.18	0.00	0.00	0.25	0.07	0.00	0.25	590	12.8	-5.5	1.8	1376	1408	8.18
FCo18	0.25	0.00	0.25	0.00	0.00	0.25	0.00	0.00	0.25	655	11.5	-6.0	2.8	1445	1449	8.25
<b>OPT.</b>																
FCo2	0.16	0.00	0.08	0.01	0.24	0.24	0.05	0.00	0.22	485	14.2	-5.8	-3.2	1212	1257	8.18
FCo10	0.18	0.00	0.09	0.00	0.25	0.25	0.06	0.00	0.17	493	14.0	-5.6	-4.0	1205	1248	8.06
FCo15	0.22	0.01	0.05	0.00	0.25	0.24	0.09	0.00	0.14	517	14.2	-5.8	-5.3	1195	1235	7.95
FCo16	0.22	0.00	0.03	0.01	0.24	0.24	0.10	0.00	0.16	523	14.1	-5.9	-4.1	1194	1233	8.07
FCo11	0.25	0.00	0.18	0.00	0.00	0.25	0.07	0.00	0.25	590	12.8	-5.5	1.8	1376	1408	8.18
FCo19	0.20	0.00	0.13	0.00	0.20	0.20	0.07	0.00	0.20	684	14.5	-6.2	-2.3	1230	1276	7.93
FCo19'	0.20	0.00	0.20	0.00	0.20	0.20	0.00	0.00	0.20	650	13.4	-5.1	-4.3	1264	1314	8.00

**Table 2**

Predicted Pareto optimal compositions ( $x_i$ ), single phase start temperature (SPST), ideal entropy of mixing ( $\Delta S_C^{id}$ ), room temperature Gibbs energy variation of the phase assemblage evolution ( $\Delta G^*$ ), enthalpy of mixing ( $\Delta H_{mix}^{FCC}$ ), solidus temperature ( $T_{solidus}$ ), liquidus temperature ( $T_{liquidus}$ ) and the corresponding valence electron concentration (VEC) of alloys formed of a single **FCC phase** within the **Fe-Al-Cr-Cu-Mn-Ni-V-Ti** system. The compositions are in mol fraction, the temperatures are in °C, the entropy in J.mol<sup>-1</sup>.K<sup>-1</sup> and both the Gibbs energy and the enthalpy are in kJ.mol<sup>-1</sup>.

#	$x_{Fe}$	$x_{Al}$	$x_{Cr}$	$x_{Cu}$	$x_{Mn}$	$x_{Ni}$	$x_V$	$x_{Ti}$	SPST	$\Delta S_C^{id}$	$\Delta G^*$	$\Delta H_{mix}^{FCC}$	$T_{solidus}$	$T_{liquidus}$	VEC
<b>T-S</b>															
F1	0.05	0.21	0.00	0.00	0.25	0.25	0.00	0.24	666	12.6	-4.0	-29.4	833	913	6.24
F2	0.06	0.20	0.00	0.02	0.24	0.25	0.01	0.22	705	13.6	-4.3	-27.7	833	919	6.41
F3	0.25	0.10	0.02	0.04	0.25	0.25	0.05	0.04	744	14.6	-6.5	-15.5	1102	1185	7.52
F4	0.24	0.11	0.04	0.04	0.24	0.25	0.05	0.03	785	14.9	-6.7	-15.5	1105	1187	7.48
F5	0.22	0.17	0.05	0.05	0.20	0.20	0.00	0.11	874	15.1	-8.9	-20.3	945	1105	6.96
<b>T-G</b>															
F1	0.05	0.21	0.00	0.00	0.25	0.25	0.00	0.24	666	12.6	-4.0	-29.4	833	913	6.24
F1*	0.03	0.23	0.00	0.00	0.24	0.25	0.00	0.25	716	12.3	-3.5	-30.6	804	892	6.11
F6	0.00	0.25	0.01	0.00	0.25	0.24	0.00	0.25	764	11.9	-3.2	-30.5	774	887	5.96
<b>T-F</b>															
F1	0.05	0.21	0.00	0.00	0.25	0.25	0.00	0.24	666	12.6	-4.0	-29.4	833	913	6.24
F7	0.25	0.06	0.09	0.04	0.25	0.25	0.06	0.00	863	14.3	-5.6	-9.6	1180	1222	7.71
<b>OPT.</b>															
F8	0.25	0.10	0.08	0.05	0.25	0.25	0.00	0.02	770	14.1	-6.2	-13.9	1142	1223	7.66
F4	0.24	0.11	0.04	0.04	0.24	0.25	0.05	0.03	785	14.9	-6.7	-15.5	1105	1187	7.48
F9	0.24	0.10	0.10	0.05	0.24	0.25	0.00	0.02	846	14.3	-5.9	-13.5	1136	1217	7.63
F7	0.25	0.06	0.09	0.04	0.25	0.25	0.06	0.00	863	14.3	-5.6	-9.6	1180	1222	7.71
F10	0.25	0.07	0.12	0.04	0.25	0.25	0.00	0.02	882	14.0	-6.1	-11.0	1153	1226	7.70

the Fe-Mn-Ni-Co (FCo1 to FCo6; FCo8) and the Fe-Mn-Ni (FCo7 to FCo9) systems which are experimentally confirmed HEAs [31]. The optimization of the second bi-objective function (T-G) allows the identification of HEA candidates derived from Fe-Cr-Ni-Co (FCo11), a system studied experimentally by Zaddach et al. [32], and other

iron-free materials: Cr-Mn-Ni-Co (FCo14; equimolar system studied by Wu et al. [37]) and Mn-Ni-V-Co-Cr (FCo12 and FCo13) alloys. To our knowledge, these are new HEA candidates never reported in the literature. The optimization of the third bi-objective function (T-F) leads to the identification of the stoichiometric FeCrNiCo alloy

which is almost at the eutectic composition ( $(T_{liquidus} - T_{solidus}) = 4^\circ\text{C}$ ).

Finally, we present two elemental substitution matrices ( $B_{FCo19}(SPST)$  and  $B_{FCo19}(SPST+100)$ ) associated with the stoichiometric FeCrMnNiCo Cantor's alloy that was also found on the Pareto front (FCo19') generated by our chemical-phase space exploration strategy. A Pareto front is the ensemble of compositions

mixing ( $\Delta S_C^{id}$ ), the room-temperature variation of Gibbs energy associated with the phase assemblage evolution  $\Delta G^*$ , the room-temperature enthalpy of mixing of the disordered solution ( $\Delta H_{mix}$ ; ref states.: pure elements in the FCC or BCC state), the solidus and liquidus temperature ( $T_{solidus}$  and  $T_{liquidus}$ ) as well as the valence electron concentration (VEC) as defined by Guo et al. [14] are given in Table 2 (target phase: disordered FCC) and Table 3

$$B_{FCo19'}(SPST) = \begin{pmatrix} +x_{Fe} & +x_{Al} & +x_{Cr} & +x_{Cu} & +x_{Mn} & +x_{Ni} & +x_V & +x_{Ti} & +x_{Co} \\ -x_{Fe} & 0 & 0 & 0.2 & 0 & 0.2 & 0 & 0 & 0 \\ -x_{Al} & 0 & 0 & 0 & 0 & 0 & 0 & 0 & 0 \\ -x_{Cr} & 0 & 0 & 0 & 0 & 0 & 0 & 0 & 0 \\ -x_{Cu} & 0 & 0 & 0.02 & 0 & 0 & 0 & 0 & 0 \\ -x_{Mn} & 0 & 0 & 0.2 & 0 & 0 & 0 & 0 & 0 \\ -x_{Ni} & 0.2 & 0 & 0.2 & 0 & 0.2 & 0 & 0 & 0 \\ -x_V & 0 & 0 & 0 & 0 & 0 & 0 & 0 & 0 \\ -x_{Ti} & 0 & 0 & 0 & 0 & 0 & 0 & 0 & 0 \\ -x_{Co} & 0.2 & 0 & 0.2 & 0 & 0.2 & 0.2 & 0 & 0 \end{pmatrix}$$
  

$$B_{FCo19'}(SPST+100) = \begin{pmatrix} +x_{Fe} & +x_{Al} & +x_{Cr} & +x_{Cu} & +x_{Mn} & +x_{Ni} & +x_V & +x_{Ti} & +x_{Co} \\ -x_{Fe} & 0 & 0 & 0.2 & 0 & 0.2 & 0.16 & 0 & 0 & 0.10 \\ -x_{Al} & 0.01 & 0 & 0.01 & 0 & 0.01 & 0.01 & 0 & 0 & 0.02 \\ -x_{Cr} & 0.03 & 0 & 0 & 0 & 0.04 & 0.02 & 0 & 0 & 0.02 \\ -x_{Cu} & 0.02 & 0 & 0.03 & 0 & 0.02 & 0.02 & 0 & 0 & 0.03 \\ -x_{Mn} & 0.1 & 0 & 0.2 & 0 & 0 & 0.07 & 0 & 0 & 0.05 \\ -x_{Ni} & 0.2 & 0 & 0.2 & 0 & 0.2 & 0 & 0 & 0 & 0.14 \\ -x_V & 0.02 & 0 & 0.09 & 0 & 0.03 & 0.02 & 0 & 0 & 0.02 \\ -x_{Ti} & 0.01 & 0 & 0.1 & 0 & 0.02 & 0.01 & 0 & 0 & 0.01 \\ -x_{Co} & 0.2 & 0 & 0.2 & 0 & 0.2 & 0.2 & 0 & 0 & 0 \end{pmatrix}$$

which simultaneously minimize and/or maximize a set of objective functions under a given set of linear or non-linear constraints as defined by the Pareto concept of optimum. (For more details on the Pareto theory see e.g Ref. [38]). The substitution matrix coefficient  $m_{ij}$  represents the mol fraction of  $i$  that can be substituted by  $j$ . In our notation,  $+x_i$  is the mol fraction added to  $i$  while  $-x_j$  is that removed from  $j$ . Note that 1) the substitution matrix is not symmetric as one can add an element not originally present in the system, and 2) the substitution matrix represents the possible substitution between two elements only. The first matrix identifies the elemental substitution that can be made in order to keep a constant SPST. This substitution matrix is of high value when trying to minimize the cost of the alloy. The second substitution matrix shows the extended degree of freedom we have when tolerating an increase of the SPST by 100 °C.

### 3.2. New low-cost first-generation HEA candidates

Following the methodology described in section 2, we evaluated optimal compositions for the Fe-Al-Cr-Cu-Mn-Ni-V-Ti system that meet the requirements of first-generation HEAs. As mentioned before, this is a low-cost system suitable for future commercial applications. The predicted optimal composition, the single phase start temperature (SPST), the ideal configurational entropy of

(target phase: disordered BCC).

More than 500 compositions were identified as HEA candidates within the Fe-Al-Cr-Cu-Mn-Ni-V-Ti system after applying Step 1 of our proposed chemical-phase space exploration strategy. These 500 compositions contain 4,5,6 and 7-component systems. Next, this initial HEA candidate list was greatly reduced by applying Step 2 of our proposed strategy (see section 2). For step 1, the optimization procedure computational time was about 8 h using a single i7 processor.

Table 2 presents 10 new first-generation HEA candidates (single phase FCC) containing 3d transition metals obtained from 3 different bi-objective function optimizations. The first observation that can be made, when comparing with the reported HEAs [5], is the deliberate absence of cobalt. According to the review of Zhang et al. [5], more than 70% of the reported FCC single-phase HEAs contain Co. In fact, Miracle and Senkov [2] reported only one 3d transition metal candidate belonging to the second generation of HEAs (multiphasic/heat treatable) that does not contain Co, i.e. the  $\text{Al}_{0.5}\text{CrCuFeNi}_2$  alloy. A recent study of Fang et al. [39] explains in detail the beneficial effect of cobalt on the mechanical properties of HEAs (Note: Section 3.1 reports HEA candidates identified using our exploration strategy for a multicomponent system that contains Co).

In this study, we explore the low-cost chemical-phase space and

**Table 3**

Predicted Pareto optimal compositions ( $x_i$ ), single phase start temperature (SPST), ideal entropy of mixing ( $\Delta S_C^{id}$ ), room temperature Gibbs energy variation of the phase assemblage evolution ( $\Delta G^*$ ), enthalpy of mixing ( $\Delta H_{mix}^{FCC}$ ), solidus temperature ( $T_{solidus}$ ), liquidus temperature ( $T_{liquidus}$ ) and the corresponding valence electron concentration (VEC) of alloys formed of a single **BCC phase** within the **Fe-Al-Cr-Cu-Mn-V-Ti** system. The compositions are in mol fraction, the temperatures are in °C, the entropy in J.mol<sup>-1</sup>.K<sup>-1</sup> and both the Gibbs energy and the enthalpy are in kJ.mol<sup>-1</sup>.

#	$x_{Fe}$	$x_{Al}$	$x_{Cr}$	$x_{Cu}$	$x_{Mn}$	$x_V$	$x_{Ti}$	SPST	$\Delta S_C^{id}$	$\Delta G^*$	$\Delta H_{mix}^{BCC}$	$T_{solidus}$	$T_{liquidus}$	VEC
<b>T-S</b>														
B1	0.00	0.25	0.25	0.00	0.25	0.25	0.00	8	11.5	0.0	-14.2	1534	1631	5.25
B2	0.25	0.25	0.07	0.00	0.18	0.25	0.00	233	12.8	-0.3	-14.8	1494	1544	5.68
B3	0.12	0.16	0.24	0.00	0.24	0.25	0.00	307	13.1	-0.7	-10.5	1548	1619	5.81
B4	0.20	0.20	0.20	0.00	0.20	0.20	0.00	363	13.5	-0.9	-11.4	1506	1568	5.80
B5	0.08	0.21	0.01	0.01	0.25	0.22	0.22	429	13.6	-1.9	-14.8	1423	1493	5.17
B6	0.23	0.25	0.01	0.01	0.16	0.19	0.15	485	13.9	-1.7	-16.9	1400	1466	5.43
B7	0.12	0.25	0.08	0.01	0.24	0.25	0.05	573	14.0	-0.9	-14.9	1457	1535	5.43
B8	0.18	0.20	0.20	0.00	0.18	0.20	0.04	621	14.2	-1.7	-11.7	1479	1561	5.66
B9	0.15	0.25	0.01	0.00	0.23	0.25	0.11	426	13.3	-1.0	-16.7	1443	1510	5.31
B10	0.14	0.21	0.11	0.02	0.16	0.13	0.23	780	15.1	-4.2	-13.1	1351	1434	5.32
B11	0.18	0.18	0.20	0.02	0.15	0.18	0.09	919	15.2	-3.6	-9.9	1403	1528	5.71
B12	0.20	0.12	0.17	0.02	0.20	0.16	0.13	964	15.3	-5.4	-7.6	1337	1464	5.92
<b>T-G</b>														
B1	0.00	0.25	0.25	0.00	0.25	0.25	0.00	8	11.5	0.0	-14.2	1534	1631	5.25
B4	0.20	0.20	0.20	0.00	0.20	0.20	0.00	363	13.5	-0.9	-11.4	1506	1568	5.80
B4*	0.19	0.12	0.18	0.01	0.19	0.17	0.14	968	15.1	-5.1	-7.9	1352	1481	5.81
<b>T-F</b>														
B1	0.00	0.25	0.25	0.00	0.25	0.25	0.00	8	11.5	0.0	-14.2	1534	1631	5.25
B13	0.02	0.23	0.25	0.00	0.25	0.25	0.00	72	12.1	0.0	-13.5	1541	1631	5.35
B14	0.25	0.25	0.00	0.00	0.25	0.25	0.00	147	11.5	0.0	-15.9	1468	1512	5.75
B15	0.25	0.17	0.11	0.00	0.22	0.25	0.00	315	13.1	-1.1	-11.1	1505	1548	5.96
B16	0.25	0.14	0.11	0.00	0.25	0.25	0.00	364	13.0	-1.6	-9.6	1497	1539	6.08
B17	0.21	0.23	0.00	0.12	0.25	0.00	0.19	852	13.2	-3.5	-14.4	1225	1247	6.20
<b>OPT.</b>														
B9	0.15	0.25	0.01	0.00	0.23	0.25	0.11	426	13.3	-1.0	-16.7	1443	1510	5.31
B6	0.23	0.25	0.01	0.01	0.16	0.19	0.15	485	13.9	-1.7	-16.9	1400	1466	5.43
B7	0.12	0.25	0.08	0.01	0.24	0.25	0.05	573	14.0	-0.9	-14.9	1457	1535	5.43
B18	0.23	0.19	0.20	0.00	0.23	0.11	0.04	698	14.0	-2.2	-10.8	1415	1488	5.93
B10	0.14	0.21	0.11	0.02	0.16	0.13	0.23	780	15.1	-4.2	-13.1	1351	1434	5.32

assume that Co is too expensive for common commercial applications. F1, an Al-Mn-Ni-Ti based material, has the lowest SPST temperature and a small driving force for the phase assemblage evolution at room temperature. This driving force can be further reduced (F6) by completely removing iron. Alloys F2 to F5 are all Fe-Mn-Ni-Al based candidates taken from the Pareto front that simultaneously minimize the SPST and maximize the ideal configurational entropy of mixing. Co (FCC phase stabilizer) is substituted by Mn in these HEA candidates. This appears to be a positive substitution as Mn improves the merits of austenitic (FCC) steels [40].

It is also interesting to note that the presence of Al in alloys F2 to F5 stabilizes the disordered FCC solid solution via the configurational entropy of mixing contribution of this solution. When Al is removed, the C14-Fe2Ti-type Laves phase forms. The elimination of this intermetallic phase appears to be beneficial as it plays an important role in the corrosion mechanism of other HEAs [41]. F1\*, an Fe-Mn-Ni based alloy with a high  $\Delta S_C^{id}$ , is the candidate with the smallest temperature range of solidification (42 °C).

Other optimal compositions (F8 to F10) that present a small SPST, low driving force for the phase assemblage evolution and limited temperature range of solidification are given in Table 2. Results presented in this table also confirm a) a certain degree of correlation between high values of  $\Delta S_C^{id}$  and the possibility of producing first-generation HEAs and b) that the magnitude of  $\Delta H_{mix}$  is around -10 kJ per mol. However, numerous HEA candidates identified in this table do not strictly follow these rules. As an example F1 has a strongly negative enthalpy of mixing ( $\Delta H_{mix} = -29.4 \text{ kJ mol}^{-1}$ ) and a small ideal configurational entropy of mixing ( $\Delta S_C^{id} = 12.6 \text{ J mol}^{-1} \text{ K}^{-1}$ ). As mentioned previously, the maximization of  $\Delta S_C^{id}$  is intended to optimize the number of heterogeneous pairs in the targeted disordered solution. As it does not completely

define the total entropy of mixing of the solution (which needs to include the effect of short-range order on the configurational entropy of mixing as well as the excess vibrational and electronic entropy contributions),  $\Delta S_C^{id}$  must not be directly correlated with the thermodynamic stability of the targeted disordered phase. Moreover, the range of temperature for which a single-phase disordered solution is stable is modulated by its Gibbs energy which is a function of both the total entropy of mixing and the enthalpy of mixing. This explains for example why different 4-component equimolar alloys (with identical values of  $\Delta S_C^{id}$ ) from the Fe-Cr-Co-Mn-Ni system possess very different single-phase start temperatures [20]. This confirms the importance of providing to the scientific community an efficient exploration composition-phase space algorithm to fine-tune the theoretical chemistry of HEA candidates based on other criteria.

Results of the application of the same search strategy for the identification of low-cost BCC first-generation HEAs are presented in Table 3. This table reveals important differences between FCC and BCC first-generation HEAs regarding the SPST (which is noticeably smaller for BCC HEAs) and the range of thermal stability (which is wider for BCC HEAs). The stoichiometric AlCrMnV alloy (B1) shows perfectly these differences: it has a SPST of 8°C and is thermodynamically stable over a range of 1526°C. Two other stoichiometric alloys, i.e. FeAlCrMnV-B4 and FeAlMnV-B14, also lie on the Pareto front.

Finally, it is to be noted that the VEC criterion established by Guo et al. is perfectly respected for all the BCC HEA candidates (i.e. VEC < 6.87). For FCC HEA candidates, the VEC criterion is also fully respected for the Co-containing alloys as Co (VEC = 9) greatly contributes to an increase of the alloy VEC. For low-cost FCC HEA candidates that do not contain Co, it seems as though the identified HEA candidates should lie, at best, in a two-phase (FCC + BCC)

**Table 4**

Predicted Pareto optimal compositions ( $x_i$ ), single phase start temperature (SPST), ideal entropy of mixing ( $\Delta S_C^{id}$ ), room temperature Gibbs energy variation of the phase assemblage evolution ( $\Delta G^*$ ), enthalpy of mixing ( $\Delta H_{mix}^{BCC}$ ), solidus temperature ( $T_{solidus}$ ), liquidus temperature ( $T_{liquidus}$ ) and the corresponding valence electron concentration (VEC) of alloys formed of a single **BCC phase** within the **Fe-Al-Cr-Cu-Mn-V-Ti-Mo** system. The compositions are in mol fraction, the temperatures are in °C, the entropy in J.mol<sup>-1</sup>.K<sup>-1</sup> and both the Gibbs energy and the enthalpy are in kJ.mol<sup>-1</sup>.

#	$x_{Fe}$	$x_{Al}$	$x_{Cr}$	$x_{Cu}$	$x_{Mn}$	$x_V$	$x_{Ti}$	$x_{Mo}$	SPST	$\Delta S_C^{id}$	$\Delta G^*$	$\Delta H_{mix}^{BCC}$	$T_{solidus}$	$T_{liquidus}$	VEC
<b>T-S</b>															
BMo1	0.07	0.18	0.02	0.02	0.24	0.21	0.23	0.03	505	14.7	-3.0	-13.7	1419	1502	5.27
BMo2	0.12	0.20	0.03	0.02	0.20	0.20	0.20	0.03	537	15.2	-3.2	-14.6	1409	1492	5.34
BMo3	0.11	0.20	0.13	0.00	0.20	0.20	0.12	0.04	564	15.4	-3.5	-12.8	1443	1536	5.38
BMo4	0.12	0.20	0.02	0.03	0.20	0.18	0.20	0.05	604	15.5	-3.5	-14.0	1400	1489	5.41
BMo5	0.12	0.21	0.00	0.09	0.13	0.20	0.14	0.11	832	15.8	-4.7	-11.1	1456	1585	5.71
BMo6	0.17	0.20	0.15	0.00	0.12	0.17	0.10	0.09	704	15.9	-5.0	-10.7	1457	1568	5.49
BMo7	0.14	0.15	0.15	0.01	0.14	0.14	0.15	0.12	796	16.5	-6.6	-7.9	1419	1563	5.58
BMo8	0.15	0.15	0.15	0.00	0.15	0.15	0.15	0.10	795	16.1	-6.1	-8.7	1419	1548	5.55
BMo9	0.14	0.17	0.09	0.06	0.16	0.08	0.20	0.10	861	16.7	-6.9	-9.2	1316	1436	5.75
<b>T-G</b>															
BMo1	0.07	0.18	0.02	0.02	0.24	0.21	0.23	0.03	505	14.7	-3.0	-13.7	1419	1502	5.27
BMo10	0.09	0.25	0.25	0.00	0.13	0.25	0.00	0.03	582	13.5	-1.0	-12.2	1568	1659	5.31
<b>T-F</b>															
BMo1	0.07	0.18	0.02	0.02	0.24	0.21	0.23	0.03	505	14.7	-3.0	-13.7	1419	1502	5.27
BMo11	0.12	0.20	0.04	0.01	0.20	0.20	0.20	0.03	543	15.1	-3.2	-14.7	1412	1494	5.29
BMo12	0.17	0.20	0.19	0.00	0.20	0.19	0.02	0.03	607	14.6	-1.9	-11.3	1486	1564	5.71
BMo13	0.24	0.20	0.00	0.02	0.25	0.18	0.07	0.04	643	14.2	-2.8	-13.2	1398	1459	5.91
BMo14	0.18	0.19	0.04	0.10	0.19	0.02	0.21	0.07	872	15.7	-6.1	-11.4	1247	1294	6.04
<b>OPT.</b>															
BMo3	0.11	0.20	0.13	0.00	0.20	0.20	0.12	0.04	564	15.4	-3.5	-12.8	1443	1536	5.38
BMo15	0.20	0.20	0.20	0.00	0.16	0.20	0.00	0.04	655	14.2	-1.8	-10.3	1521	1590	5.76
BMo15	0.13	0.20	0.00	0.09	0.15	0.17	0.14	0.12	826	16.0	-5.0	-10.6	1428	1559	5.81
BMo17	0.18	0.19	0.04	0.10	0.19	0.02	0.21	0.07	872	15.7	-6.1	-11.4	1247	1294	6.04
BMo-0-Fe	0.00	0.25	0.00	0.09	0.17	0.21	0.14	0.14	610	14.5	-4.2	-11.8	1473	1665	5.38

region according to the VEC criterion. This intriguing result needs to be further explored.

### 3.3. Mo-based first-generation HEAs

In order to examine the advantages of adding a refractory material with an intermediate price, as defined by Fu et al. [8], we also considered the addition of molybdenum (~5USD/mole) to the Fe-Al-Cr-Mn-V-Ti based alloys. These last HEA candidates as identified in this work are presented in Table 4. This table presents the BCC single-phase first-generation HEA with the largest number of components ever reported, i.e. the 7-component FeAlCrMnVTiMo<sub>2/3</sub> alloy (BMo8). In the steel metallurgy literature it is well known that all these elements, with the exception of Mn, are ferrite-BCC-stabilizers. In this specific case, it is interesting to note that the complete removal of Mn from this system would lead to the following phase equilibrium modifications: an increase of 100°C of both the liquidus and the solidus combined with a change of the SPST to 737°C. Mn is introduced in the system mainly to

maximize the ideal configurational entropy of mixing of the BCC phase. We can further increase this energetic contribution by adding a minor Cu addition (see BMo9).

When considering other thermodynamic criteria (see T-G and T-F results) for the composition optimization, these two candidates would not be optimal. For that reason it would be highly interesting to study experimentally the mechanical and chemical behavior of these two candidates in the future to see if an alloy design based on the maximization of the ideal configurational entropy of mixing is useful.

Finally, in matrix  $B_{BMo8}(SPST)$  we show the substitutional matrix for the BMo8 candidate. This is the largest BCC disordered region identified in this work. Again, this matrix is of high value when trying to substitute different elements based on their price without changing a targeted critical value (the SPST value in this example). The large number of non-zero values in this substitutional matrix and the fact that the values are quite large show a wide range of stability of the BCC phase for this alloy.

$$B_{BMo8}(SPST) = \begin{pmatrix} +x_{Fe} & +x_{Al} & +x_{Cr} & +x_{Cu} & +x_{Mn} & +x_V & +x_{Ti} & +x_{Mo} \\ -x_{Fe} & 0 & 0.02 & 0.15 & 0 & 0.08 & 0.05 & 0.15 & 0.05 \\ -x_{Al} & 0.15 & 0 & 0.15 & 0 & 0.15 & 0.15 & 0.15 & 0.1 \\ -x_{Cr} & 0.15 & 0.02 & 0 & 0 & 0.15 & 0.1 & 0.15 & 0.08 \\ -x_{Cu} & 0.03 & 0.02 & 0.04 & 0 & 0.03 & 0.03 & 0.02 & 0.03 \\ -x_{Mn} & 0.15 & 0.02 & 0.15 & 0 & 0 & 0.15 & 0.15 & 0.1 \\ -x_V & 0.15 & 0.04 & 0.15 & 0 & 0.15 & 0 & 0.15 & 0.1 \\ -x_{Ti} & 0.15 & 0.02 & 0.15 & 0 & 0.15 & 0.08 & 0 & 0.1 \\ -x_{Mo} & 0.11 & 0.03 & 0.06 & 0 & 0.15 & 0.06 & 0.06 & 0 \end{pmatrix}$$

#### 4. Conclusion

In this study, an original method to predict the composition and the temperature range of stability of first-generation high entropy alloys has been proposed. This method is based on the ability of the CALPHAD method to predict complex phase equilibria of multicomponent systems and uses an optimization algorithm, the Mesh Adaptive Direct Search algorithm, to calculate the optimal compositions in a reasonable computation time. This method can be applied to find potential HEAs in other systems under various sets of compositions and thermophysical property constraints, even if the constraints are non-linear and non-smooth, as the MADS algorithm is specifically designed to solve such problems.

The application of this method to the low cost Fe-Al-Cr-Cu-Mn-Ni-V-Ti system, with a current price of less than 0.5 USD/mol, has led to the identification of entire sets of new FCC and BCC HEA candidates. Moreover, the optimization of new bi-objective functions based on the SPST, the room temperature driving force for precipitation and the solidification range shows the possibility of fine-tuning the chemistry of HEAs to optimal values. We have also observed a certain correlation between the ideal configurational entropy of mixing and the tendency to form first-generation HEAs. The logical continuation of this work is to study experimentally the various low-cost HEA candidates identified in this work that would support or undermine the reliability of the database and the method of determination of HEA candidates via the proposed optimization procedure.

#### Acknowledgements

This research was supported by funds from the Natural Sciences and Engineering Research Council of Canada (NSERC) through the Discovery Grant of Prof. Harvey.

#### Appendix - Two-phases heavily alloyed HEAs

In this appendix, we present two examples illustrating the capability of our method for tuning the microstructure of a two-phase HEA.

In the first example, different mol fractions of the B2 ordered phase precipitating in the disordered BCC matrix at room temperature are targeted. The algorithm can be described as follows:

1. Maximize the activity  $a$  of both BCC and B2 phases until they become stable, i.e.  $a_{BCC} = a_{B2} = 1$
2. Starting from an initial composition  $(x_0, T_0)$  for which  $a_{BCC} = a_{B2} = 1$ , minimize the two objective functions:  $\|X_{B2} - X_{B2}^0\|_2$  ( $X_{B2}^0$  being the targeted value of the B2 phase fraction) and amount (mole fraction) of all other phases except single phase BCC and B2
3. Maximize the ideal configurational entropy of mixing

In the second example, the same strategy is employed to identify microstructures with equimolar fractions of FCC and BCC disordered phases.

**Table A1**

Predicted Pareto optimal compositions ( $x_i$ ) maximizing the ideal entropy of mixing ( $\Delta S_C^{id}$ ) for alloys formed of two phases: disordered **single BCC phase** plus a target phase fraction of **single B2 phase** within the Fe-Al-Cr-Cu-Mn-Ni-V-Ti system. The compositions are in mol fraction, and the entropy in J.mol<sup>-1</sup>.K<sup>-1</sup>. The valence electron concentration (VEC) is reported for comparison with the phase stability criterion of Guo et al. [14].

#	$x_{Fe}$	$x_{Al}$	$x_{Cr}$	$x_{Cu}$	$x_{Mn}$	$x_{Ni}$	$x_V$	$x_{Ti}$	$X_{B2}$	$\Delta S_C^{id}$	VEC
<b><math>X_{B2} \approx 0.2</math></b>											
T-P1	0.18	0.18	0.18	0.00	0.16	0.16	0.14	0.00	0.196	14.57	6.48
$X_{B2} \approx 0.15$											
T-P-2	0.20	0.20	0.09	0.00	0.18	0.13	0.20	0.00	0.150	14.73	6.3
T-P-3	0.10	0.20	0.20	0.00	0.10	0.20	0.20	0.00	0.158	14.82	6.3
<b><math>X_{B2} \approx 0.10</math></b>											
T-P-4	0.20	0.16	0.20	0.00	0.12	0.12	0.20	0.00	0.100	14.53	6.32
T-P-5	0.10	0.20	0.20	0.00	0.11	0.19	0.20	0.00	0.100	14.75	6.27
T-P-6	0.01	0.20	0.20	0.00	0.20	0.19	0.20	0.00	0.081	14.59	6.18
<b><math>X_{B2} \approx 0.05</math></b>											
T-P-7	0.20	0.20	0.20	0.00	0.20	0.00	0.20	0.00	0.041	14.24	5.8

**Table A2**

Predicted Pareto optimal compositions ( $x_i$ ) maximizing the ideal entropy of mixing ( $\Delta S_C^{id}$ ) for alloys formed of two **single BCC phase** and **single FCC phase** in equal proportion (~ 50% – 50%) within the Fe-Al-Cr-Cu-Mn-Ni-V-Ti system. The compositions are in mol fraction, and the entropy in J.mol<sup>-1</sup>.K. The valence electron concentration (VEC) is reported for comparison with the phase stability criterion of Guo et al. [14].

#	$x_{Fe}$	$x_{Al}$	$x_{Cr}$	$x_{Cu}$	$x_{Mn}$	$x_{Ni}$	$x_V$	$x_{Ti}$	$X_{BCC}$	$\Delta S_C^{id}$	VEC
B-F-1	0.13	0.01	0.16	0.18	0.19	0.19	0.14	0.00	0.518	15.13	7.94
B-F-2	0.19	0.04	0.20	0.00	0.20	0.19	0.16	0.02	0.497	14.76	7.02

#### References

- [1] R. Kirchheim, B. Heine, H. Fischmeister, S. Hofmann, H. Knote, U. Stoltz, The passivity of iron-chromium alloys, Corrosion Sci. 29 (7) (1989) 899–917. [https://doi.org/10.1016/0010-938X\(89\)90060-7](https://doi.org/10.1016/0010-938X(89)90060-7). <http://www.sciencedirect.com/science/article/pii/0010938X89900607>.
- [2] D. Miracle, O. Senkov, A critical review of high entropy alloys and related concepts, Acta Mater. 122 (2017) 448–511. <https://doi.org/10.1016/j.actamat.2016.08.081>. <http://www.sciencedirect.com/science/article/pii/S1359645416306759>.
- [3] M.-H. Tsai, J.-W. Yeh, High-entropy alloys: a critical review, Mater. Res. Lett. 2 (3) (2014) 107–123.
- [4] Y. Ye, Q. Wang, J. Lu, C. Liu, Y. Yang, High-entropy alloy: challenges and prospects, Mater. Today 19 (6) (2016) 349–362. <https://doi.org/10.1016/j.mattod.2015.11.026>. <http://www.sciencedirect.com/science/article/pii/S1369702115004010>.
- [5] M. Gao, J. Yeh, P. Liaw, Y. Zhang, High-entropy Alloys: Fundamentals and Applications, Springer International Publishing, 2016. <https://doi.org/10.1007/978-3-319-27013-5>. <https://books.google.ca/books?id=hDvtjgEACAAJ>.
- [6] M. C. G. R. Feng, P. K. Liaw, M. Widom, First-principles prediction of high-entropy-alloy stability, NPJ Comput. Mater. 50.
- [7] H.L. Lukas, S.G. Fries, B. Sundman, et al., Computational Thermodynamics: the Calphad Method, vol. 131, Cambridge university press, Cambridge, 2007.
- [8] X. Fu, C. Schuh, E. Olivetti, Materials selection considerations for high entropy alloys, Scripta Mater. 138 (2017) 145–150. <https://doi.org/10.1016/j.scriptamat.2017.03.014>. <http://www.sciencedirect.com/science/article/pii/S1359646217301392>.
- [9] C.W. Bale, E. Bélistre, P. Chartrand, S. Deckerov, G. Eriksson, A.E. Gheribi, K. Hack, I.-H. Jung, Y.-B. Kang, J. Melanor, A.D. Pelton, S. Petersen, C. Robelin, J. Sangster, P. Spencer, M.-A.V. Ende, FactSage thermochemical software and databases, 20102016, Calphad 54 (2016) 35–53, <https://doi.org/10.1016/j.calphad.2016.05.002>, <http://www.sciencedirect.com/science/article/pii/S0364591616300694>.
- [10] S. Le Digabel, Algorithm 909: NOMAD: nonlinear optimization with the MADS algorithm, ACM Trans. Math. Software 37 (4) (2011) 44:1–44:15, <https://doi.org/10.1145/1916461.1916468>. <https://doi.org/10.1145/1916461.1916468>.
- [11] A. Abu-Odeh, E. Galvan, T. Kirk, H. Mao, Q. Chen, P. Mason, R. Malak, R. Arryave, Efficient exploration of the high entropy alloy composition-phase

- space, *Acta Mater.* 152 (2018) 41–57. <https://doi.org/10.1016/j.actamat.2018.04.012>. <http://www.sciencedirect.com/science/article/pii/S1359645418302854>.
- [12] Y. Zhang, T.T. Zuo, Z. Tang, M.C. Gao, K.A. Dahmen, P.K. Liaw, Z.P. Lu, Microstructures and properties of high-entropy alloys, *Prog. Mater. Sci.* 61 (2014) 1–93. <https://doi.org/10.1016/j.pmatsci.2013.10.001>. <http://www.sciencedirect.com/science/article/pii/S0079642513000789>.
- [13] Y. Zhang, Y. Zhou, J. Lin, G. Chen, P. Liaw, Solid-solution phase formation rules for multi-component alloys, *Adv. Eng. Mater.* 10 (6) (2008) 534–538, <https://doi.org/10.1002/adem.200700240>, <https://doi.org/10.1002/adem.200700240>.
- [14] S. Guo, C. Ng, J. Lu, C.T. Liu, Effect of valence electron concentration on stability of fcc or bcc phase in high entropy alloys, *J. Appl. Phys.* 109 (10) (2011) 103505, <https://doi.org/10.1063/1.3587228>.
- [15] J.-P. Harvey, G. Eriksson, D. Orban, P. Chartrand, Global minimization of the gibbs energy of multicomponent systems involving the presence of order/disorder phase transitions, *Am. J. Sci.* 313 (3) (2013) 199–241, <https://doi.org/10.2475/03.2013.02>.
- [16] R. Kikuchi, S.G. Brush, Improvement of the cluster variation method, *J. Chem. Phys.* 47 (1) (1967) 195–203, <https://doi.org/10.1063/1.1711845>, <https://doi.org/10.1063/1.1711845>.
- [17] W.A. Oates, F. Zhang, S.-L. Chen, Y.A. Chang, Improved cluster-site approximation for the entropy of mixing in multicomponent solid solutions, *Phys. Rev. B* 59 (1999) 11221–11225, <https://doi.org/10.1103/PhysRevB.59.11221>. <https://link.aps.org/doi/10.1103/PhysRevB.59.11221>.
- [18] Factsage software and database description, URL <http://www.factsage.com/>.
- [19] B. Cantor, I. Chang, P. Knight, A. Vincent, Microstructural development in equiatomic multicomponent alloys, *Mater. Sci. Eng., A* 375–377 (2004) 213–218. <https://doi.org/10.1016/j.msea.2003.10.257>. <http://www.sciencedirect.com/science/article/pii/S0921509303009936>.
- [20] G. Bracq, M. Laurent-Brocq, L. Perrière, R. Pirs, J.-M. Joubert, I. Guillot, The fcc solid solution stability in the co-cr-fe-mn-ni multi-component system, *Acta Mater.* 128 (2017) 327–336. <https://doi.org/10.1016/j.actamat.2017.02.017>. <http://www.sciencedirect.com/science/article/pii/S1359645417301088>.
- [21] F. Otto, A. Dlouh, C. Somsen, H. Bei, G. Eggeler, E. George, The influences of temperature and microstructure on the tensile properties of a co-crfe-mnni high-entropy alloy, *Acta Mater.* 61 (15) (2013) 5743–5755. <https://doi.org/10.1016/j.actamat.2013.06.018>. <http://www.sciencedirect.com/science/article/pii/S1359645413004503>.
- [22] R. Kozak, A. Sologubenko, W. Steurer, Single-phase high-entropy alloys—an overview, *Z. für Kristallogr. - Cryst. Mater.* 230 (1) (2015) 55–68.
- [23] C. Audet, J.E. Dennis Jr., Mesh adaptive direct search algorithms for constrained optimization, *SIAM J. Optim.* 17 (1) (2006) 188–217, <https://doi.org/10.1137/040603371>.
- [24] C. Audet, W. Hare, Derivative-free and Blackbox Optimization, Springer Series in Operations Research and Financial Engineering, Springer International Publishing, 2017, <https://doi.org/10.1007/978-3-319-68913-5>, <https://doi.org/10.1007/978-3-319-68913-5>.
- [25] A.E. Gheribi, J.-P. Harvey, E. Béolis, C. Robelin, P. Chartrand, A.D. Pelton, C.W. Bale, S. Le Digabel, Use of a biobjective direct search algorithm in the process design of material science applications, *Optim. Eng.* 17 (1) (2016) 27–45, <https://doi.org/10.1007/s11081-015-9301-2>. <https://doi.org/10.1007/s11081-015-9301-2>.
- [26] A.E. Gheribi, C. Audet, S. Le Digabel, E. Béolis, C.W. Bale, A.D. Pelton, Calculating optimal conditions for alloy and process design using thermodynamic and property databases, the FactSage software and the mesh adaptive direct search algorithm, *Calphad* 36 (2012) 135–143. <https://doi.org/10.1016/j.calphad.2011.06.003>. <http://www.sciencedirect.com/science/article/pii/S0364591611000563>.
- [27] A.E. Gheribi, S. Le Digabel, C. Audet, P. Chartrand, Identifying optimal conditions for magnesium based alloy design using the mesh adaptive direct search algorithm, *Thermochim. Acta* 559 (2013) 107–110. <https://doi.org/10.1016/j.tca.2013.02.004>. <http://www.sciencedirect.com/science/article/pii>
- S0040603113000816.
- [28] A.E. Gheribi, C. Robelin, S. Le Digabel, C. Audet, A.D. Pelton, Calculating all local minima on liquidus surfaces using the factsage software and databases and the mesh adaptive direct search algorithm, *J. Chem. Therm.* 43 (9) (2011) 1323–1330. <https://doi.org/10.1016/j.jct.2011.03.021>. <http://www.sciencedirect.com/science/article/pii/S0021961411001005>.
- [29] E. Béolis, Z. Huang, S. Le Digabel, A.E. Gheribi, Evaluation of machine learning interpolation techniques for prediction of physical properties, *Comput. Mater. Sci.* 98 (2015) 170–177. <https://doi.org/10.1016/j.commatsci.2014.10.032>. <http://www.sciencedirect.com/science/article/pii/S092702561400706X>.
- [30] J.-P. Harvey, A.E. Gheribi, Process simulation and control optimization of a blast furnace using classical thermodynamics combined to a direct search algorithm, *Metall. Mater. Trans. B* 45 (1) (2014) 307–327, <https://doi.org/10.1007/s11663-013-0004-9>. <https://doi.org/10.1007/s11663-013-0004-9>.
- [31] Z. Wu, H. Bei, G. Pharr, E. George, Temperature dependence of the mechanical properties of equiatomic solid solution alloys with face-centered cubic crystal structures, *Acta Mater.* 81 (2014) 428–441. <https://doi.org/10.1016/j.actamat.2014.08.026>. <http://www.sciencedirect.com/science/article/pii/S1359645414006272>.
- [32] A. Zaddach, R. Scattergood, C. Koch, Tensile properties of low-stacking fault energy high-entropy alloys, *Mater. Sci. Eng., A* 636 (2015) 373–378. <https://doi.org/10.1016/j.msea.2015.03.109>. <http://www.sciencedirect.com/science/article/pii/S092150931500369X>.
- [33] B. Gludovatz, A. Hohenwarter, D. Catoo, E.H. Chang, E.P. George, R.O. Ritchie, A fracture-resistant high-entropy alloy for cryogenic applications, *Science* 345 (6201) (2014) 1153–1158, <https://doi.org/10.1126/science.1254581>, arXiv: <http://science.sciencemag.org/content/345/6201/1153.full.pdf>.
- [34] A. Gali, E. George, Tensile properties of high- and medium-entropy alloys, *Intermetallics* 39 (2013) 74–78. <https://doi.org/10.1016/j.intermet.2013.03.018>. <http://www.sciencedirect.com/science/article/pii/S0966979513000903>.
- [35] M.S. Lucas, L. Mauger, J.A. Muoz, Y. Xiao, A.O. Sheets, S.L. Semiatin, J. Horwath, Z. Turgut, Magnetic and vibrational properties of high-entropy alloys, 07E307, *J. Appl. Phys.* 109 (7) (2011), <https://doi.org/10.1063/1.3538936>, <https://doi.org/10.1063/1.3538936>.
- [36] M.-H. Chuang, M.-H. Tsai, W.-R. Wang, S.-J. Lin, J.-W. Yeh, Microstructure and wear behavior of alxco1.5crfe1.5tiy high-entropy alloys, *Acta Mater.* 59 (16) (2011) 6308–6317. <https://doi.org/10.1016/j.actamat.2011.06.041>. <http://www.sciencedirect.com/science/article/pii/S1359645411004551>.
- [37] Z. Wu, H. Bei, F. Otto, G. Pharr, E. George, Recovery, recrystallization, grain growth and phase stability of a family of fcc-structured multi-component equiatomic solid solution alloys, *Intermetallics* 46 (2014) 131–140. <https://doi.org/10.1016/j.intermet.2013.10.024>. <http://www.sciencedirect.com/science/article/pii/S0966979513002872>.
- [38] P. Godfrey, R. Shipley, J. Gryz, Algorithms and analyses for maximal vector computation, *The VLDB Journal* 16 (1) (2007) 5–28, <https://doi.org/10.1007/s00778-006-0029-7>. <https://doi.org/10.1007/s00778-006-0029-7>.
- [39] W. Fang, R. Chang, X. Zhang, P. Ji, X. Wang, B. Liu, J. Li, X. He, X. Qu, F. Yin, Effects of cobalt on the structure and mechanical behavior of non-equal molar cofe50xcr25ni25 high entropy alloys, *Mater. Sci. Eng., A* 723 (2018) 221–228. <https://doi.org/10.1016/j.msea.2018.01.029>. <http://www.sciencedirect.com/science/article/pii/S0921509318300297>.
- [40] S.-T. Chen, W.-Y. Tang, Y.-F. Kuo, S.-Y. Chen, C.-H. Tsau, T.-T. Shun, J.-W. Yeh, Microstructure and properties of age-hardenable alxcrfe1.5mnni0.5 alloys, *Mater. Sci. Eng., A* 527 (21) (2010) 5818–5825. <https://doi.org/10.1016/j.msea.2010.05.052>. <http://www.sciencedirect.com/science/article/pii/S0921509310005769>.
- [41] Z. Cai, X. Cui, G. Jin, Z. Liu, N. Tan, Y. Li, M. Dong, D. Zhang, Effect of v content on microstructure and properties of laser-solidified fe60(nicrcoivx)40 (x=0, 0.5, 1) multicomponent alloy coatings on aisi 1045 steel, *Mater. Char.* 132 (2017) 373–380. <https://doi.org/10.1016/j.matchar.2017.09.007>. <http://www.sciencedirect.com/science/article/pii/S1044580317322131>.